

# Quantitative Interpretation of the Response of Surface Plasmon Resonance Sensors to Adsorbed Films

Linda S. Jung,<sup>†</sup> Charles T. Campbell,<sup>\*,†</sup> Timothy M. Chinowsky,<sup>‡</sup>  
Mimi N. Mar,<sup>‡</sup> and Sinclair S. Yee<sup>‡</sup>

Chemistry Department and Electrical Engineering Department, University of Washington,  
Seattle, Washington 98195-2500

Received November 11, 1997. In Final Form: March 30, 1998

A simple but quantitative mathematical formalism for interpretation of surface plasmon resonance (SPR) signals from adsorbed films of a wide variety of structures is presented. It can be used to estimate adsorbed film thicknesses, surface coverages, or surface concentrations from the SPR response over the entire range of film thicknesses without relying on calibration curves of response versus known thicknesses or surface concentrations. This formalism is compared to more complex optical simulations. It is further tested by (1) calibrating the response of two SPR spectrometers to changes in bulk index of refraction, (2) using these calibrations with this formalism to predict responses to several well-characterized adlayer structures (alkanethiolates and serum albumin on gold, propylamine on COOH-functionalized gold), and then (3) comparing these predictions to measured SPR responses. Methods for estimating the refractive index of the adlayer material are also discussed. Detection limits in both bulk and adsorption-based analyses are discussed. The planar system used here has a detection limit of  $\sim 0.003$  nm in average film thickness for adsorbates whose refractive index differs from that of the solvent by only 0.1. The temperature sensitivities of these two SPR spectrometers are characterized and discussed in terms of detection limits.

## I. Introduction

Sensors based upon surface plasmon resonance (SPR) spectroscopy are becoming increasingly popular due to their high sensitivity and simple construction.<sup>1–16</sup> SPR-based sensors can detect refractive index (RI) changes smaller than  $10^{-5}$  with a time resolution of a few seconds (e.g., see ref 14 and data presented below). Because it senses with an evanescent wave, an SPR sensor responds to the RI of its analyte only to a depth of  $\sim 200$  nm from the sensor surface. This allows SPR sensors to be applied to the detection of adsorption onto the sensor surface from liquid solutions,<sup>1–14,16</sup> even in a microscopic mode with  $\sim 5$

$\mu\text{m}$  lateral resolution.<sup>17</sup> The binding of an adsorbate to the metal surface of the SPR sensor, or to an immobilized functionalization layer on that metal surface, may be monitored in real time if the adsorbate has a different refractive index than the bulk solution. If the sensor surface is functionalized to contain selective receptors for specific chemicals or biomolecules, selective chemical and biochemical sensors can be constructed. SPR spectroscopy also has many potential applications in fundamental surface science, since it is one of the few techniques that can directly detect adsorption onto a surface immersed in liquid with high time resolution and submonolayer sensitivity.

To apply SPR sensing to the monitoring of adsorption processes, some method must be available to extract from the SPR sensor response a quantitative measurement of the thickness or surface concentration of the adsorbed layer. However, despite the wide application of SPR, no simple yet general method for predicting the response of an SPR sensor to a given adsorbate has been published. It is the main purpose of this paper to present a new, simple, but quantitative mathematical formalism for interpretation of SPR signals from adsorbed films of a wide variety of structures. We will also test this formalism by (1) calibrating the response of two SPR spectrometers to changes in bulk index of refraction, (2) using these calibrations with this formalism to predict responses to several well-characterized adlayer structures, and then (3) comparing these predictions to measured SPR responses. We supplement these thin adlayer experiments with optical simulations of the sensor response to the growth of thicker films. We will also discuss methods for characterizing SPR detection limits in both bulk and adsorption-based analyses and present these for the two SPR systems used here. Finally, we will characterize the temperature sensitivities of these two SPR spectrometers and discuss how they affect detection limits.

\* Corresponding author.

<sup>†</sup> Chemistry Department.

<sup>‡</sup> Electrical Engineering Department.

(1) Lundstrom, I. *Biosens. Bioelectron.* **1994**, *9*, 725.

(2) Lukosz, W. *Biosens. Bioelectron.* **1997**, *12*, 175.

(3) Melendez, J.; Carr, R.; Bartholomew, D.; Taneja, H.; Sixth International Conference on Chemical Sensors (Washington, D.C.), Development of a surface plasmon resonance sensor for commercial applications, 1996.

(4) Melendez, J.; Carr, R.; Bartholomew, D. U.; Kukanskis, K.; Elkind, J.; Yee, S.; Furlong, C.; Woodbury, R. *Sens. Actuators, B* **1996**, *35*, 212.

(5) Kooyman, R. P. H.; Kolkman, H.; Gent, J. V.; Greve, J. *Anal. Chim. Acta* **1988**, *213*, 35.

(6) Stenberg, E.; Persson, B.; Roos, H.; Urbaniczky, C. *J. Colloid Interface Sci.* **1991**, *143*, 513.

(7) O'Shannessy, D. J. *Curr. Opin. Biotechnol.* **1994**, *5*, 65.

(8) Liedberg, B.; Lundstrom, I.; Stenberg, E. *Sens. Actuators, B* **1993**, *11*, 63.

(9) Liedberg, B.; Nylander, C.; Lundström, I. *Biosens. Bioelectron.* **1995**, *10*, 1.

(10) Mrksich, M.; Grunwell, J. R.; Whitesides, G. M. *J. Am. Chem. Soc.* **1995**, *117*, 12009.

(11) Mrksich, M.; Sigal, G. B.; Whitesides, G. M. *Langmuir* **1995**, *11*, 4383.

(12) Mrksich, M.; Whitesides, G. M. *Annu. Rev. Biophys. Biomol. Struct.* **1996**, *25*, 55.

(13) Peterlinz, K. A.; Georgiadis, R. *Langmuir* **1996**, *12*, 4731.

(14) Kunz, U.; Katerkamp, A.; Renneberg, R.; Spener, F.; Cammann, K. *Sens. Actuators, B* **1996**, *32*, 149.

(15) Yeatman, E. M. *Biosens. Bioelectron.* **1996**, *11*, 635.

(16) Pharmacia, *BIAcore System Manual*; Pharmacia Biosensor AB, Scientific Information: Uppsala, Sweden, 1991.

(17) Haeussling, L.; Ringsdorf, H.; Schmitt, F.-J.; Knoll, W. *Langmuir* **1991**, *7*, 1837.

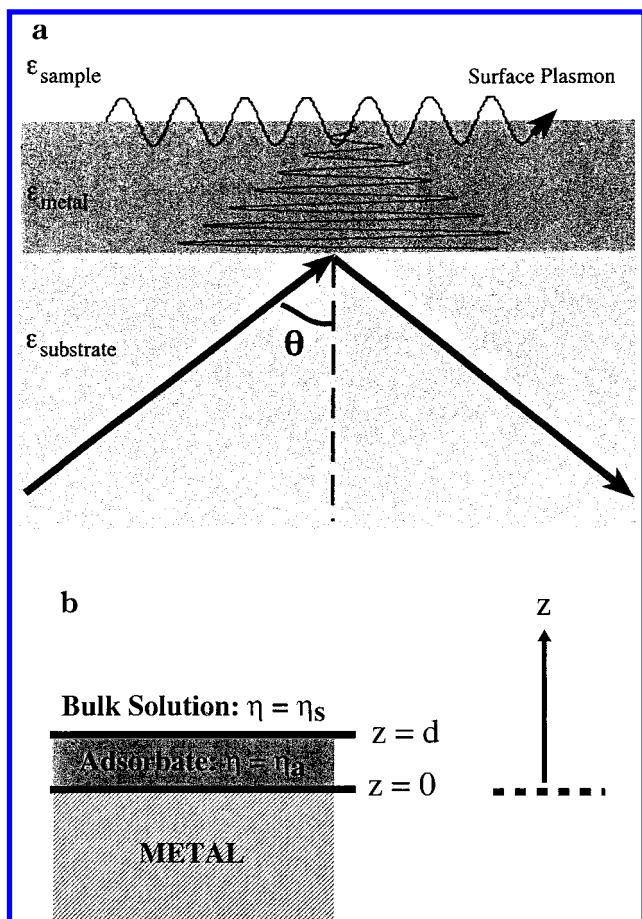


**Figure 1.** (a) Schematic diagram of the working interface of an SPR spectrometer and the SPR effect. The working interface involves a thin metal film on a transparent substrate, in contact with a medium to be probed, usually a liquid solution. (b). Schematic diagram of a bilayer structure involving an adsorbate **a** of thickness  $d$  and refractive index  $\eta_a$  directly on the metal probe surface, above which is solution **s**, of refractive index  $\eta_s$ .

An SPR sensor consists of a transparent optical substrate coated with a thin ( $\sim 50$  nm) metal film (see Figure 1, for example). Here the metal is gold, but silver is also often used. The fluid medium (here a liquid solution) to be analyzed is in contact with the metal surface, and adsorption can take place from this solution onto the metal surface. Often the metal is purposefully coated with something else, so that the adsorption sites are not necessarily metal sites. Light passes through the substrate and reflects from the interface between the substrate and the analyte medium at an incident angle or range of angles greater than the critical angle. One then measures the specularly reflected light intensity. Depending on the spectrometer, one can either use monochromatic light, in which case one monitors intensity versus incident angle, or a white light, in which case one measures intensity versus wavelength at a fixed angle. For certain wavelengths and angles of incident light, part of the incident energy will couple into a surface plasmon wave traveling along the interface between the gold layer and the solution to be analyzed. The loss of this energy is observed as a sharp attenuation of reflectivity, known as the surface plasmon resonance effect. The angles and wavelengths at which this occurs vary extremely sensitively with the refractive index (RI) (or complex dielectric constant) of the medium in contact with the metal surface of the SPR sensor.<sup>2,8,18–20</sup>

The sensor response is characterized by the wavelength  $\lambda$  or angle  $\theta$  of minimum reflectivity. Shifts in these quantities ( $\Delta\lambda$  or  $\Delta\theta$ ) thus yield measurements of changes in the RI,  $\Delta\eta$ , of the medium to be interrogated. That medium need not have a uniform RI, but instead may have a more complex structure, such as an adsorbed film in a liquid solution (Figure 1b). The sensor response thus reflects some sort of an *average* RI. The way this averaging occurs is a major subject of this paper. We will show that the thickness of an adlayer or the surface concentration of an adsorbate can be determined by matching the predicted “average” RI for a given thickness or surface concentration with that actually measured by the SPR sensor.

Several papers have previously addressed some aspects of the quantitative interpretation of SPR signals in terms of adlayer structural parameters.<sup>2,5–8,13,15–17,20–23</sup> Most of these addressed quantitative analysis of adsorbed films that are much thinner than the decay length of the evanescent field, in the so-called linear-response regime. Stenberg et al.<sup>6</sup> used full numerical simulations of Maxwell’s equations for thin-film structures to show that a nearly linear response is obtained versus surface concentration of adsorbed proteins and confirmed this by radiolabeling experiments. Kooyman et al.<sup>5</sup> similarly calculated thicknesses from the measured response to protein adsorption using Maxwell’s (Fresnel) equations and showed it to agree with the dimensions of the protein molecule. Liedberg et al.<sup>8</sup> measured a linear response to surface concentration of adsorbed proteins (in  $\text{ng}/\text{mm}^2$ ) with a slope that was nearly independent of the protein. Peterlinz et al.<sup>13</sup> calculated film thicknesses (versus their dielectric constant) from the measured SPR response to a monolayer of adsorbed alkanethiols and from this showed how to determine fractional adsorbate coverages from the response at lower coverages. In general, these papers show that quantitative estimates of adlayer film thickness or adsorbate coverage can be determined in this linear regime if a calibration curve is first made wherein the response is plotted versus known thicknesses or surface concentrations. Such a linear calibration curve is the method generally used with commercial instruments<sup>16</sup> and is based on a model by Sjölander et al.<sup>24</sup> It can only be used in studying the same adsorbate or adsorbates that have similar dielectric properties to that used in generating the calibration plot.

A few papers have addressed the response to thicker films, beyond the linear regime. Liedberg et al.<sup>8</sup> showed through Maxwell’s (Fresnel) equations that the SPR response to local changes in the index of refraction decays exponentially with distance from the surface with a characteristic decay length equal to one-half that for the decay of the evanescent field. Lukosz<sup>2,20</sup> used a perturbation theory approach on Maxwell’s equations to calculate the effective refractive index of uniform adlayers, showing that this varied linearly with film thickness for small thicknesses but showed increasing nonlinearity at high thicknesses. He similarly showed how to estimate the effects of any anisotropy of the optical properties of the adlayer.

(18) Sambles, J. R.; Bradbery, G. W.; Yang, F. *Contemp. Phys.* **1991**, *32*, 173.

(19) Barker, A. S. *Phys. Rev. B: Solid State* **1973**, *8*, 5418.

(20) Lukosz, W. *Biosens. Bioelectron.* **1991**, *6*, 215.

(21) Hanken, D. G.; Corn, R. M. *Anal. Chem.* **1995**, *67*, 3767.

(22) Silin, V. I.; Balchytis, G. A.; Yakovlev, V. A. *Opt. Commun.* **1993**, *97*, 19.

(23) Silin, V.; Weetall, H.; Vanderah, D. J. *J. Colloid Interface Sci.* **1997**, *185*, 94.

(24) Sjölander, S.; Urbaniczky, C. *Anal. Chem.* **1991**, *63*, 2338.

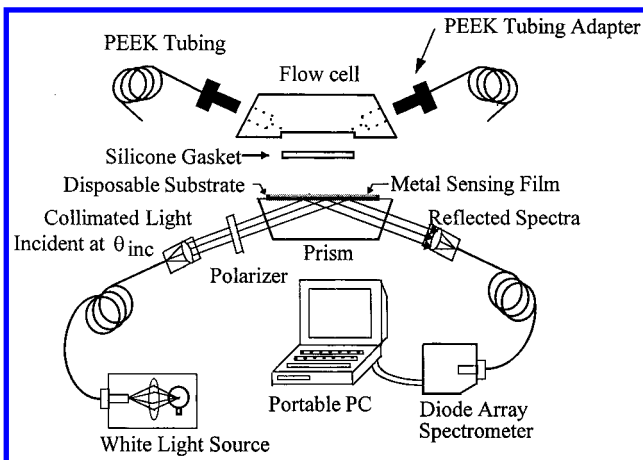


**Figure 2.** Schematic diagram of the planar SPR spectrometer and flow cell system.

Here, we will show how to estimate adsorbed film thicknesses, surface coverages, or surface concentrations from the SPR response without relying on calibration curves of response versus known thicknesses or surface concentrations. Such surface-based calibration curves are very difficult to make. Here, we will show how to use a much simpler calibration curve: SPR response versus bulk refractive index. We will also show how to apply this simpler calibration over the entire surface concentration range, from the linear-response regime of small thicknesses up to films thicker than the decay length of the evanescent field.

A method for estimating the refractive index of the adlayer will also be discussed here that relies on knowledge of the composition of the adsorbate. More complex SPR measurements using more than one color<sup>25,26</sup> or detailed line shape analysis<sup>27</sup> have recently been suggested that potentially give information on both the film thickness and the index of refraction of the adsorbate. Those will not be discussed here, since this paper focuses on simpler sensors wherein only the SPR minimum (wavelength or angle) is monitored.

## II. Experimental Section

**Sensor Platforms.** We used two SPR sensing systems: a planar device and a fiber optic device. Both systems use a white-light source incident at angles fixed by the detector geometry. Reflected light was measured using a photodiode array spectrometer (Ocean Optics, Inc., model S1000); each spectrum was then manipulated by computer to find the wavelength of minimum reflection. Both systems used  $\sim 50$  nm electron-beam-evaporated gold layers on top of a 2 nm chromium adhesion layer.

**Planar Sensor.** In the planar device, Figure 2, the gold SPR sensing surface is deposited onto a glass microscope slide that is then index-matched to a prism. The collimated white light source is directed with a fiber optic through the prism and this glass slide to impinge onto the gold sensing surface at an angle of  $78^\circ$  from normal, and the specularly reflected light exiting the prism is collected into a fiber optic jumper cable that directs it into a diode array spectrometer for analysis. (The incident light is linear transverse-magnetic-polarized, so that its magnetic field is parallel to the gold surface.) A flow cell is mounted onto the sensor/prism assembly so that solutions of sensing interest can be introduced easily to flow across the gold surface and switching between different solutions can be accomplished rapidly. To provide better temperature stability and control, the optical

system is fixed to an aluminum mount and enclosed in a thermally insulated box.

**Fiber Optic Sensor.** The fiber optic SPR sensor is described elsewhere<sup>28</sup> and consists of a  $\sim 15$  cm length of 400  $\mu\text{m}$  diameter optical fiber, one end of which has been stripped of 10 mm of its jacket and optical cladding. A gold film is evaporated onto the surface of the cylindrical stripped region, forming the SPR sensor surface. A gold mirror ( $\sim 150$  nm thick) is deposited onto the polished flat end of the stripped end of the fiber. The other end of the fiber is mounted in a fiber-optic connector.

White light travels down the fiber and strikes the SPR sensing surface at a range of angles fixed by the modal distribution of the fiber. The reflected light strikes the mirror on the end of the fiber and bounces back up the fiber into the spectrometer.

The probe senses the RI of whatever medium surrounds its sensing surface. The probe was not used in a flow cell; instead, the probe tip was immersed in a beaker of analyte, and the solution in the beaker was changed (for example, by adding solute or solvent). Due to the temperature sensitivity of the index of refraction of solutions, it is important to keep its temperature constant (see below).

**Prefunctionalized Gold Films.** The gold surfaces were sometimes prefunctionalized with alkanethiolate or  $-\text{COOH}$  terminated alkanethiolate adlayers according to previous literature<sup>29–34</sup> as described next.

The gold-coated glass microscope slides were cleaned in basic peroxide solution (a 1:1:5 solution of  $\text{NH}_4\text{OH}$ , 30% by volume  $\text{H}_2\text{O}_2$ , and deionized water<sup>35</sup>). The slides were placed in the solution and heated to  $40$ – $70^\circ\text{C}$  for about 5 min. The samples were then removed, rinsed thoroughly with deionized water (during which it was tested for hydrophilicity), rinsed with ethanol, and dried with  $\text{N}_2$ . The gold films were then placed in a jar containing 1.0–0.1 mM solution of the corresponding thiol in degassed ( $\text{N}_2$ ) absolute ethanol. The jar was flushed with  $\text{N}_2$  and then sealed (with the lid and Parafilm). The samples were left in the solution for 24–72 h to build the thiolate adlayer and then removed and rinsed with ethanol to remove excess and weakly bound thiols before use.

The gold-coated fiber-optics probes were first cleaned by sequential soaking for several minutes in boiling solvents (toluene, octane, *n*-hexane, absolute ethanol, and deionized water), rinsed with absolute ethanol, and then dried with  $\text{N}_2$ . Immediately after drying, the probes were put in a 1 mM solution of the corresponding thiol in absolute ethanol in a (Handi-wrap or Parafilm) covered beaker for 16–72 h to build the thiolate adlayer and then removed and rinsed with ethanol to remove excess and weakly bound thiols before use.

**Bulk Solutions.** The index of refraction of the various bulk solutions (sucrose/water, ethanol/water, toluene/ethanol) was measured with an Abbe-3L refractometer (Milton Roy Co., Rochester, NY).

## III. SPR Response to Bulk Solutions: Measured Calibration Plots

Let us first define the SPR response as either the shift in wavelength ( $\Delta\lambda$ ) or angle ( $\Delta\theta$ ) of the SPR minimum in reflected light intensity associated with changes in the index of refraction of the medium in contact with the metal surface of the SPR device,  $\Delta n$ . We have frequently measured the SPR response to changes in the *bulk* index of refraction of solutions in contact with the gold surface

(28) Jorgenson, R. C.; Yee, S. S. *Sens. Actuators* **1993**, B12, 213.

(29) Bain, C. D.; Evall, J.; Whitesides, G. M. *J. Am. Chem. Soc.* **1989**, 111, 7155.

(30) Bain, C. D.; Whitesides, G. M. *J. Am. Chem. Soc.* **1989**, 111, 7164.

(31) Bain, C. D.; Troughton, E. B.; Tao, Y.-T.; Evall, J.; Whitesides, G. M.; Nuzzo, R. G. *J. Am. Chem. Soc.* **1989**, 111, 321.

(32) Allara, D. L. *Biosens. Bioelectron.* **1995**, 10, 771.

(33) DeBono, R. F.; Loucks, G. D.; Della Manna, D.; Krull, U. J. *Can. J. Chem.* **1996**, 74, 677.

(34) Dubois, L. H.; Nuzzo, R. G. *Annu. Rev. Phys. Chem.* **1992**, 43, 437.

(35) Perrson, N. O.; Uvdal, K.; Liegberg, B.; Hellsten, M. *Prog. Colloid Polym. Sci.* **1992**, 88, 100.

(25) Peterlinz, K. A.; Georgiadis, R. *Opt. Commun.* **1996**, 130, 260.

(26) Johnston, K. S.; Karlson, S. R.; Jung, C. C.; Yee, S. S. *Mater. Chem. Phys.* **1995**, 42, 242.

(27) Ehler, T. T.; Malmberg, N.; Noe, L. J. *J. Phys. Chem. B* **1997**, 101, 1268.



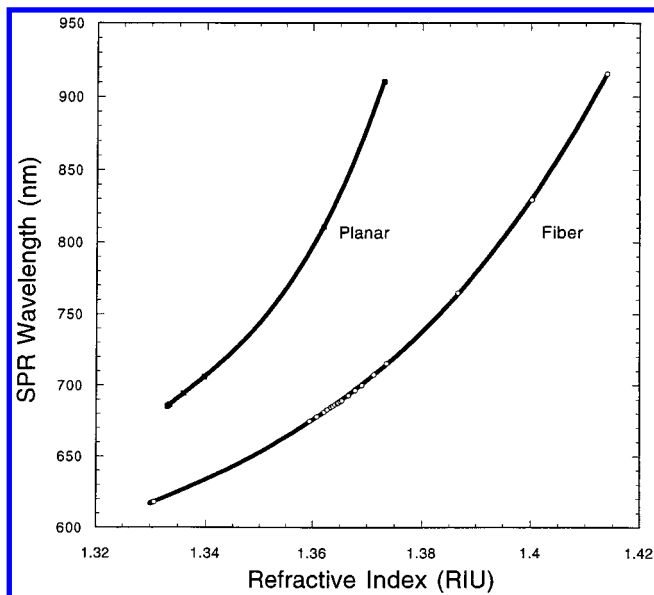


**Figure 3.** Measured SPR response (wavelength of minimum in the reflected light intensity) versus the bulk index of refraction ( $\eta$ ) of solutions in contact with the gold SPR probe surface, for both the planar and fiber-optic SPR spectrometers, shown over a broad range of  $\eta$ .

for both of the SPR systems of this study. Some typical calibration plots are shown in Figure 3, for both the planar and fiber-optic SPR probes. The wavelength of the SPR minimum is plotted versus refractive index of the solution in contact with the gold, using several different binary solutions (sucrose/water, ethanol/water, toluene/ethanol), each with a range of concentrations. For these solutions, the change in wavelength due to differences in adsorption between different solutions should be very small compared to the measured shifts, which are dominated by changes in the bulk index of refraction of these solutions. As can be seen, the response in all cases is fairly linear over a narrow enough RI range, but curvature is obvious when viewing the broader index range available. (Note that this upward curvature is predicted by Maxwell's equations in simulations such as those below.) Similar results have been reported previously.<sup>8</sup> Thus, over a narrow range, the response to changes in bulk index of refraction, in the absence of adsorption from the solution, can be approximated as linear:

$$R = m \Delta\eta = m(\eta_{\text{final}} - \eta_{\text{initial}}) \quad (1a)$$

The magnitude of the local slope,  $m$ , in any small range of indices can be thought of as a sensitivity factor for the sensor. To make the units on this slope clearer for the reader, we refer here to a "refractive index unit" or RIU. While this is unnecessary since the refractive index is really unitless, we believe it makes the paper easier to follow.

Figure 4 shows a plot of the wavelength of the SPR minimum for the planar system over a much smaller range of index of refraction near 1.335 RIU, collected over a narrower time range (several hours) to minimize drift. Linearity as in eq 1a with slope 3400 nm/RIU is obvious. Returning to Figure 3, this sensitivity factor, or local slope, varies from  $\sim 3100$  to  $8800$  nm/RIU with increasing index of refraction for the planar system, and from  $\sim 1600$  to  $6000$  nm/RIU for the fiber-optic probe. Note that these slopes depend on the gold film thickness and other system parameters, and so they should be measured regularly

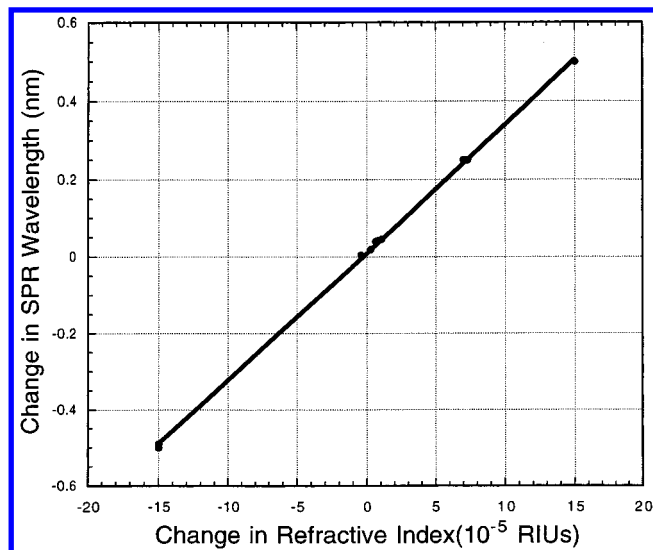


**Figure 4.** Same as Figure 3, except over a narrow range of  $\eta$  near that for water (1.330), and only for the planar system. Slope = 3450 nm/RIU.

using a few points. The observation of a reasonable slope also provides an easy means for verifying an instrument's integrity.

As described in more detail below, the curvature in such calibration plots could be explicitly incorporated into a low-order polynomial equation, for example by adding a second term to eq 1a,  $m_2 \Delta\eta^2$ , which would be negligible for small  $\Delta\eta$ :

$$R = m_1 \Delta\eta + m_2 \Delta\eta^2 \quad (1b)$$

#### IV. Calculating the SPR Response to Adsorbed Films

**IV.1. The SPR Response to a Single Adlayer of Uniform Thickness.** First consider the idealized bilayer structure in Figure 1b, wherein a thin adsorbed film of uniform thickness  $d$  and index of refraction  $\eta_a$  is bonded to the metal surface of an SPR probe. Above this adsorbate layer is a bulk liquid solution of index  $\eta_s$ . What should the SPR response be for such a structure?

In this case we define the SPR response,  $R$ , as either the shift in wavelength ( $\Delta\lambda$ ) or angle ( $\Delta\theta$ ) of the SPR minimum in reflected light intensity associated with this adsorption starting from the clean metal in contact with the same bulk solution, with no intermediate adlayer. If one could determine some effective index of refraction for the bilayer,  $\eta_{\text{eff}}$ , which would be the properly weighted average of  $\eta_a$  plus  $\eta_s$ , then one could simply estimate the response to adsorption (i.e., the change in position of the SPR minimum upon adsorption) using eq 1a or 1b. Thus, the estimated response would just be

$$R = m(\eta_{\text{eff}} - \eta_s) \quad (2a)$$

or

$$R = m_1(\eta_{\text{eff}} - \eta_s) + m_2(\eta_{\text{eff}} - \eta_s)^2 \quad (2b)$$

depending upon whether one is using the linear or quadratic calibration plot.

In eqs 2,  $\eta_{\text{eff}}$  must be the properly weighted average of  $\eta_a$  plus  $\eta_s$ . Since light is being used to probe this index of refraction, it is natural to assume that the proper weighting factor at each point in the bilayer structure should be proportional to the intensity of light at that

point. The evanescent electromagnetic field decays away exponentially into this medium with a characteristic decay length,  $l_d$ , of  $\sim 25\text{--}50\%$  of the wavelength of the light.<sup>2,8,20,36</sup> (The wavelength is typically  $\sim 500\text{--}900$  nm at the SPR minimum.) The intensity of light is the field strength squared, so it decays with height  $z$  above the metal surface as  $[\exp(-z/l_d)]^2$ . Thus, the proper weighting factor in calculating this average refractive index should just be  $[\exp(-z/l_d)]^2 = \exp(-2z/l_d)$ . This was indeed proven to be very accurate through Maxwell's equations by Liedberg et al.<sup>8</sup> Thus, the effective index of refraction is calculated by averaging the index of refraction over the depth of the whole bilayer structure, always weighting the local index with this factor. This average is therefore calculated with the depth integral:

$$\eta_{\text{eff}} = (2/l_d) \int_0^{\infty} \eta(z) \exp(-2z/l_d) dz \quad (3)$$

where  $\eta(z)$  is the index of refraction at height  $z$ . This equation is not restricted to the bilayer structure and should be generally useful even for much more complex multilayer structures. It is very different than the model used by Sjölander et al.,<sup>24</sup> which assumes unity weighting factor within the penetration depth of the evanescent wave and zero beyond.

For the bilayer structure of Figure 1b,  $\eta(z) = \eta_a$  for  $0 < z < d$ , and  $\eta(z) = \eta_s$  for  $d < z < \text{infinity}$ . In this simple case the integral of eq 3 reduces to

$$\begin{aligned} \eta_{\text{eff}} &= \eta_a [1 - \exp(-2d/l_d)] + \eta_s \exp(-2d/l_d) \\ &= \eta_s + (\eta_a - \eta_s) [1 - \exp(-2d/l_d)] \end{aligned} \quad (4)$$

A similar functional dependence on film thickness to eq 4 has been proven through a perturbation theory approach from Maxwell's equations by Lukosz.<sup>2</sup> Also, a similar approach to eqs 3 and 4 has been suggested for optical waveguide sensors,<sup>37</sup> although the decay length suggested there is twice what we propose below.

If using a linear calibration plot of response versus bulk RI, then eq 2a applies and by substituting eq 4 for  $\eta_{\text{eff}}$  one gets from it the sensor response

$$R = m(\eta_{\text{eff}} - \eta_s) = m(\eta_a - \eta_s) [1 - \exp(-2d/l_d)] \quad (5a)$$

Behavior qualitatively similar to eq 5a has been predicted based on calculations using Maxwell's equations by Liedberg et al.<sup>8</sup> A similar exponential dependence to eq 3 has been previously assumed for the effect of mass loading of receptors versus depth within a dextran coating on an SPR sensor, although in that case no connection was made to refractive index and no method for absolute quantitative calibration or estimating the decay length was proposed.<sup>38</sup> Our present results substantiate the assumptions in that paper.

In Figure 5 we plot as the solid curve the SPR response (in this case the angle of the reflection minimum at a fixed wavelength of 825 nm) predicted by eq 5a as a function of adlayer thickness calculated for a particular value of  $m$ ,  $\eta_a$  and  $\eta_s$ , and  $l_d$ . We also present there as dots the results of a much more complex calculation of the sensor response versus thickness from a thin-film optical model based on Maxwell's equations, similar to the

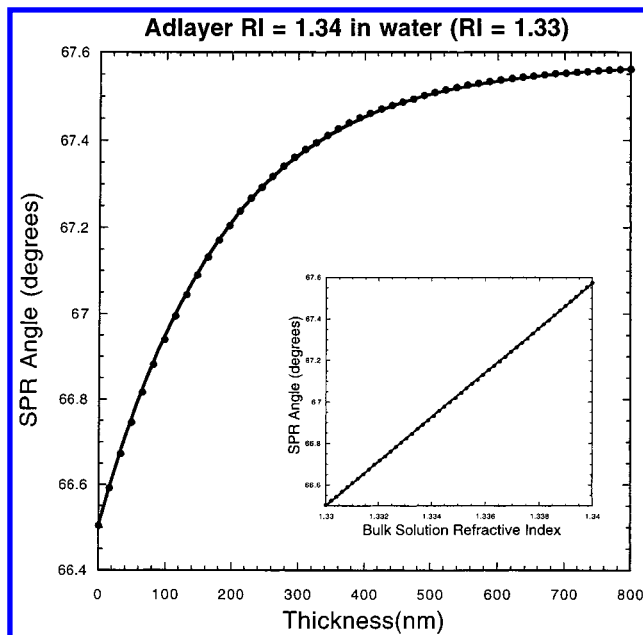


**Figure 5.** Calculated SPR response versus adlayer thickness,  $d$ , for the bilayer structure of Figure 1b, for the special case where  $\eta_a = 1.330$ ,  $\eta_s = 1.340$ , and  $\lambda = 825$  nm. Dots: full calculation with Maxwell's equations and thin-film optical model. Solid curve: calculation using eq 5a, letting  $l_d$  be 368 nm to achieve the best fit to the dotted curve. INSERT: Calculated SPR response versus bulk index of refraction, for the special case where  $\lambda = 825$  nm: dots, full calculation with Maxwell's equations and the same thin-film optical model; solid curve, the best fit of eq 1a to the dotted curve in the range from  $\eta = 1.330$  to 1.340, giving  $m = 107^\circ$  per RIU.

methods described in refs 5, 6, 8, and 39. This calculation was for a planar multilayer consisting of a glass substrate, supporting a 1 nm thick chromium layer and then a 50 nm thick gold layer, and it used the same values for  $\eta_a$  and  $\eta_s$  and light wavelength as used in eq 5a. Note that the value of  $m$  used in eq 5a as plotted here,  $107^\circ$  per RIU, was chosen to reproduce the response to bulk solutions, calculated with Maxwell's equations, and the same optical model, as shown in the insert of Figure 5. This is exactly how  $m$  would be determined experimentally: by calibrating the measured sensor response to changes in bulk refractive index as outlined above. The value of  $l_d$  (368 nm) was treated as a fitting parameter in eq 5a.

Note the excellent agreement in Figure 5 between the full calculation of Maxwell's equations and the far simpler eq 5a. This verifies the validity of eqs 3–5a, and the assumptions used in deriving them. Also note that the best-fit value of  $l_d$  (368 nm) is in the range between  $1/2$  to  $1/4$  the wavelength of light used to probe the SPR minimum, as expected based on the characteristic decay length of the evanescent field.<sup>2,8,20,36</sup> In the calculations with Maxwell's equations, we also calculated  $l_d$  for these conditions, and we found it to range from 370 to 320 nm with increasing refractive index (adlayer thickness). These values encompass the single value of  $l_d$  determined from fitting eq 5a to the more complex calculations.

The above development assumed that the SPR response was proportional to the change in bulk refractive index over the range between  $\eta_s$  and  $\eta_{\text{eff}}$ . If this is not the case, one can use the more complex nonlinear calibration curve, eq 1b, to replace eq 1a for bulk solutions, in which case

(36) Kurosawa, K.; Pierce, R. M.; Ushioda, S.; Hemminger, J. C. *Phys. Rev. B* **1986**, *33*, 789.

(37) Ramsden, J. J.; Li, S.-Y.; Prenosil, J. E.; Heinzel, E. *Biotechnol. Bioeng.* **1994**, *43*, 939.

(38) Schuck, P. *Biophys. J.* **1996**, *70*, 1230.

(39) Heavens, O. S.; *Optical Properties of Thin Films*; Dover: New York, 1955.

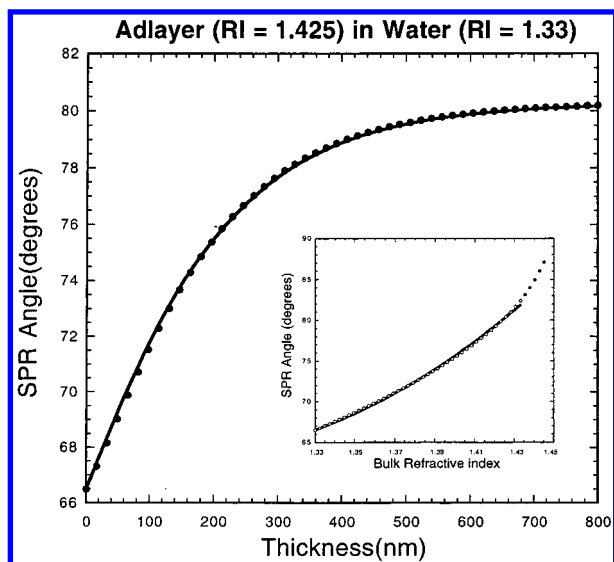


**Figure 6.** Calculated SPR response versus adlayer thickness,  $d$ , for the bilayer structure of Figure 1b, for the special case where  $\eta_a = 1.330$ ,  $\eta_s = 1.425$ , and  $\lambda = 825$  nm: dots, full calculation with Maxwell's equations and thin-film optical model; solid curve, calculation using eq 5b, letting  $l_d$  be 307 nm to achieve the best fit to the dotted curve. INSERT: Calculated SPR response versus bulk index of refraction of a pure, homogeneous solution in contact with the metal surface, for the special case where  $\lambda = 825$  nm: dots, full calculation with Maxwell's equations and the same thin-film optical model; solid curve, the best fit of eq 2b to the dotted curve in the range from  $\eta = 1.330$  to 1.433, giving  $m_1 = 89.7^\circ$  per RIU and  $m_2 = 980^\circ$  per RIU<sup>2</sup>.

the response to an adlayer is given by eq 2b. Upon substitution of eq 4 for the effective refractive index of the bilayer into eq 2b, we have

$$R = m_1(\eta_a - \eta_s)[1 - \exp(-2d/l_d)] + m_2\{(\eta_a - \eta_s)[1 - \exp(-2d/l_d)]\}^2 \quad (5b)$$

The constants  $m_1$  and  $m_2$  would be determined from the calibration curve, fitting the response to the index of bulk solutions with the quadratic eq 1b.

Equation 5b should be used in place of eq 5a whenever there is substantial nonlinearity in the SPR response to changes in the bulk refractive index in the range between  $\eta_s$  and  $\eta_{\text{eff}}$ , which generally occurs when their difference is large. Figure 6 shows that it gives an excellent fit to the solution of Maxwell's equations under such situations, again using the optical model described above and again a light wavelength of 825 nm. The geometry was the same as used in Figure 5, with the only difference being the much larger difference between  $\eta_a$  and  $\eta_s$  here. The constants  $m_1$  and  $m_2$  were again determined from a theoretical calibration curve, fitting eq 2b to the SPR response to bulk solutions calculated with Maxwell's equations, using a series of hypothetical bulk solutions covering the range between  $\eta_a$  and  $\eta_s$  here. This fit is shown as an insert to Figure 6 and gave values of  $m_1 = 89.7^\circ$  per RIU and  $m_2 = 980^\circ$  per RIU<sup>2</sup>. Note that this is exactly what would be done experimentally to get  $m_1$  and  $m_2$ . The best-fit value of  $l_d$  for eq 5b in Figure 6 was 307 nm, again within the expected range of  $1/2 - 1/4$  of the light's wavelength. The good fit further verifies eqs 3–5b. Note that the value of  $l_d$  found here is  $\sim 20\%$  lower than the value determined by the fit to eq 5a in Figure 5, 368 nm. This is consistent with the value of  $l_d$  found from our optical calculations, which decreased more dramatically, from 370 to 220 nm with increasing refractive index in this range.

When the SPR response to changes in bulk index of refraction cannot be well fitted by eq 1a or 1b, respectively, then one can certainly expect substantial errors in the above methods.

**IV.1.1. Estimation of Adsorbate Film Thickness from Measured SPR Response.** Equation 5a or 5b can be used to estimate an adlayer thickness from a measured SPR response as well as to predict the response from a certain adlayer structure. Note that the constant  $m$  in eq 5a or  $m_1$  and  $m_2$  in eq 5b would be determined first from calibration curves using bulk solutions of the type presented in Figures 3 and 4. The index of refraction of the bulk solution,  $\eta_s$ , can be either obtained from prior measurements (see, for example, ref 40) or measured, as we have done on a standard Abbe refractometer. We present below methods for estimating  $\eta_a$  if it cannot be determined by these methods. The value of  $l_d$  can be roughly estimated as  $0.37 \pm 0.13$  the light wavelength (see above), but better methods are discussed below. Thus, eq 5a or 5b above can be used to predict the SPR response to an adlayer of a certain thickness or, conversely, to estimate the adlayer thickness from the measured SPR response. Equation 5a can be rearranged to solve for the adlayer thickness

$$d = -(l_d/2) \ln(1 - R/R_{\text{max}}) \quad (6a)$$

where  $R_{\text{max}}$  is the maximum response that would be measured for an infinitely thick adlayer, or

$$R_{\text{max}} = m(\eta_a - \eta_s) \quad (6b)$$

Note that  $R_{\text{max}}$  could be directly measured in some cases, but in most cases (such as for protein or thiol adsorption, see below) it is just calculated from eq 6b as the calibration slope  $m$  times the difference between the refractive indices of the adsorbate and solvent.

In the special case where  $d$  is very small compared to  $l_d$ , eq 6a reduces to

$$d = (l_d/2)(R/R_{\text{max}}) = (l_d/2)\{R/[m(\eta_a - \eta_s)]\} \quad (7)$$

so that the response is directly proportional to the thickness of the adlayer. This is what we will call the "linear response regime". The linear response to film thickness or adsorbate surface coverage has been predicted and observed in many papers where the adsorbate was not too thick.<sup>2,5,6,8,13,16,20</sup>

In using eqs 5–7 to calculate film thickness, the absolute accuracy will only be as good as this estimate of  $l_d$ , which is only  $\pm 35\%$  in the absence of some calibration or better means of estimating it (which we will discuss below). The precision, however, is within a few percent, as seen by the quality of the fit to eqs 5a and 5b. Inaccuracy can also arise if the value of  $m$  or  $\eta_a$  used is inaccurate. At small thicknesses, the relative error in  $m$  or  $(\eta_a - \eta_s)$  directly appears as the same relative error in the thickness. The relative error due to these grows rapidly as the true thickness increases to values near  $l_d/2$ . For example, the error in thickness is 35% for a 20% error at a thickness of  $0.35l_d$ .

**IV.1.2. Estimation of Adsorbate Coverage from Measured SPR Response.** Once the average thickness,  $d$ , of a uniformly spread adlayer is estimated by the above procedure, it is a trivial matter to convert this to surface concentration,  $\theta$ , in molecules per cm<sup>2</sup>. The conversion factor is just the bulk number density of the adsorbate,

(40) Lide, D. R. Ed. *Handbook of Chemistry Physics*, 71st ed.; CRC Press: Boston, 1990.



$N$ , in units of molecules per  $\text{cm}^3$ :

$$\theta \text{ (in molecules/cm}^2\text{)} = d \text{ (in cm)} \times N \text{ (in molecules/cm}^3\text{)} \quad (8)$$

The bulk number density of the adsorbate,  $N$ , can be estimated from the bulk density of the adsorbate,  $\rho$ , in units of  $\text{g/cm}^3$  just by dividing by the molecular weight and multiplying by Avogadro's number. The proper value of  $\rho$  to use is the value for pure, condensed bulk adsorbate, which is the same material whose index of refraction  $\eta_a$  was used in eq 6, 7, or 5b to get  $d$ . If the adsorbate is a molecular fragment, its density can be estimated from that of similar molecules. (See next section for suggestions on how to choose similar molecules.)

**IV.1.3. Estimating the Refractive Index of an Adsorbate,  $\eta_a$ .** How does one determine  $\eta_a$ , the adsorbate's RI? If the adsorbate is a molecule that can be assumed to be relatively unperturbed upon adsorption, the appropriate value for  $\eta_a$  is just the index of refraction of the molecule in pure, condensed form, which can also usually be found (see ref 40) or measured. Most proteins, for example, have an index of refraction near 1.6,<sup>41</sup> and this is not expected to be perturbed much upon adsorption since the molecule is so big relative to the fraction of it that would actually form bonds to the surface. If it is a molecule or fragment of a molecule whose refractive index cannot be measured, it can be estimated based on values for molecules with similar structure. For example, adsorbed alkanethiolates on gold can be expected to have a very similar RI to the corresponding thiol, since the H atom that is lost upon adsorption occupies such a tiny fraction of the molecular volume. Similarly, adsorbed alkyls, carboxylates, or ammonium cations could be estimated from the corresponding alkane, carboxylic acid, or amine, respectively.

A more complex method of estimating refractive indices is based on the Clausius–Mossotti Equation,<sup>42</sup> which for a sample of pure compound  $j$  is

$$(\eta_j^2 - 1)/(\eta_j^2 + 2) = N_{j,0}A_j/(3\epsilon_0) \quad (9)$$

Here  $\eta_j$  is its RI,  $\epsilon_0$  is the permittivity of vacuum,  $N_{j,0}$  is the number density (number of molecules of  $j$  per unit volume in pure  $j$ ), and  $A_j$  is the frequency-dependent polarizability of the molecule. First let us consider a fluid solution. For a mixture of compound  $j$  with  $k$ , each with number densities  $N_j$  and  $N_k$ , one can estimate the index of refraction of the solution,  $\eta_{\text{soln}}$ , using the same formula, but replacing  $\eta_j$  with  $\eta_{\text{soln}}$ , and  $N_{j,0}A_j$  with the sum  $N_jA_j + N_kA_k$ . If the solution is ideal, then  $N_j = f_jN_{j,0}$ , where  $f_j$  is the volume fraction of  $j$  (i.e., the fraction of its volume occupied by  $j$ ), and likewise for  $k$ . Using eq 9 to express  $A_j$  and  $A_k$  in terms of  $\eta_j$  and  $\eta_k$ , respectively, gives the Lorenz–Lorentz equation<sup>43,44</sup>

$$(\eta_{\text{soln}}^2 - 1)/(\eta_{\text{soln}}^2 + 2) = f_j[(\eta_j^2 - 1)/(\eta_j^2 + 2)] + f_k[(\eta_k^2 - 1)/(\eta_k^2 + 2)] \quad (10a)$$

This turns out to give a nearly linear variation in the RI of the solution with the fraction of its volume occupied by

$k$ , so that the following is true to within a few percent when  $\eta_j$  and  $\eta_k$  are both within the usual range of SPR applications (from 1.33 to 1.6)

$$\eta_{\text{soln}} = f_j\eta_j + f_k\eta_k = f_j(\eta_j - \eta_k) + \eta_k \quad (10b)$$

Equation 10a can be applied to determine the RI of molecules by measuring the contribution they make to the RI of a bulk solution. For example, the addition of most proteins to aqueous buffer solution (0.3 M NaCl) causes the RI to increase by  $1.8 \times 10^{-4}$  RIU for every g/L of added protein.<sup>41</sup> (Glycoproteins and lipoproteins have somewhat lower increases.<sup>41</sup>) The specific volume of proteins in aqueous buffer is  $\sim 0.77$  mL/g.<sup>45,46</sup> Using this in eq 10b gives that  $\eta_{\text{protein}} - \eta_{\text{buffer}} = 0.234$  RIU. Since in those solutions  $\eta_{\text{buffer}} = 1.336$  RIU, we get that  $\eta_{\text{protein}} = 1.57$  RIU for the water-free protein. A nearly identical value was obtained from eq 10a in ref 43, where it was also shown that  $\eta_{\text{protein}}$  varies weakly with the wavelength of light. These values are also very close to the index of refraction measured for crystalline proteins, 1.60 RIU.<sup>24,41</sup> They are greater than the refractive index that is estimated for “adsorbed protein films” using ellipsometric approaches that assume a single optical thickness, since the film volume includes a great deal of water (see below and refs 17 and 47). Here, we are instead just referring to that part of such films which are made of protein material itself, not water. We believe this approach, which neglects the intermixed solvent in the adlayer, is more direct and general for quantitative analysis of adsorbate coverages for proteins and adsorbates in general.

Equation 10 can also be applied as an approximation in estimating the index of refraction of a sample of a single molecule (or adsorbed molecular fragment) whose value is unknown. The molecule can be separated into parts whose indices of refraction are known, and the index of refraction of the groups can be summed after scaling each with a weighting factor equal to the fraction of the molecule's volume that is occupied by that group. The RIs of groups can be estimated from applying the formula to molecules of known RI. For example, the RI of  $\text{CH}_3(\text{CH}_2)_4\text{CH}_3$  is 1.3751 and that of  $\text{CH}_3(\text{CH}_2)_{16}\text{CH}_3$  is 1.4390.<sup>40</sup> Assuming that a  $\text{CH}_2$  group and a  $\text{CH}_3$  group occupy the same volume, the above equation gives that  $\eta_{\text{CH}_2}$  and  $\eta_{\text{CH}_3}$  equal to 1.471 and 1.183, respectively. Using these group values in the same equation predicts the correct RIs for  $\text{CH}_3(\text{CH}_2)_4\text{CH}_3$  and  $\text{CH}_3(\text{CH}_2)_8\text{CH}_3$ , 1.375 and 1.41, respectively.<sup>40</sup> This also explains why the RIs of long chain alkyls, whether they be thiols, alcohols, or carboxylic acids, all approach that for the corresponding alkane as the chain length increases.<sup>40</sup> Similar analysis using the shorter chain molecules can give the group contribution from the functional group. The volume of a functional group can be estimated from its geometry (bond lengths, angles) and van der Waals radii of its atoms, or it can be treated as a parameter and determined by fitting the equation to known RIs.

One can also measure  $\eta_a$  in cases where very thick adlayers can somehow be grown. By simply measuring the maximum response for an infinitely thick ( $\gg l_d$ ) adlayer, one gets  $R_{\text{max}} = m(\eta_a - \eta_s)$ . Since the slope of the calibration plot,  $m$ , and the RI of the solvent are known, one can solve for  $\eta_a$ .

Note also that analysis of the SPR response at two wavelengths or the SPR line shape can give estimates for

(41) Armstrong, S. H., Jr.; Budka, M. J. E.; Morrison, K. C.; Hasson, M. J. *Am. Chem. Soc.* **1947**, *69*, 1747.

(42) Levine, I. N. *Physical Chemistry*; McGraw-Hill: New York, 1988.

(43) McMeekin, T. L.; Groves, M. L.; Hipp, N. J. *Adv. Chem. Ser. No.* **1964**, *44*, 54.

(44) Doty, P.; Geiduschek, E. P. In *The Proteins*; Bailey, H. N. A. K., Academic Press: New York, 1953; p 1A.

(45) Darnell, J. E.; Lodish, H.; Baltimore, D. *Molecular Cell Biology*; Scientific American Books: New York, 1990.

(46) Leslie, T. E.; Lilley, T. H. *Biopolymers* **1985**, *24*, 695.

(47) Gölander, C.-G.; Kiss, E. J. *Colloid Interface Sci.* **1988**, *121*, 240.

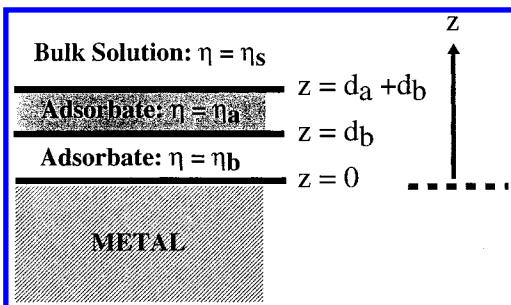


**Figure 7.** Schematic diagram of the trilayer structure involving a preadsorbate layer **b** of thickness  $d_b$  directly functionalizing the metal probe surface, above which is a second adsorbate layer **a** of thickness  $d_a$  and finally the bulk solution **s**.

both the adlayer thickness *and* its effective index of refraction (see Introduction).

**IV.1.4. Estimating the Decay Length,  $l_d$ .** The decay length,  $l_d$ , is a key parameter in these calculations. The probe depth of the technique is one-half this decay length. A rough but reasonable estimate is that  $l_d$  equals  $37 \pm 13\%$  of the light wavelength at the SPR minimum,  $\lambda$ , (see above), which for a typical minimum of 680 nm in aqueous solutions gives a probe depth  $l_d/2 = \sim 120$  nm.

A more accurate estimate of  $l_d$  comes from the Maxwell's equations, by which<sup>26</sup>

$$l_d = (\lambda/2\pi) / \text{Re}\{[\eta_{\text{eff}}^2 \epsilon_{\text{metal}} / (\eta_{\text{eff}}^2 + \epsilon_{\text{metal}})] - \eta_{\text{eff}}^2\}^{1/2} \\ = (\lambda/2\pi) / \text{Re}\{-\eta_{\text{eff}}^4 / (\eta_{\text{eff}}^2 + \epsilon_{\text{metal}})\}^{1/2} \quad (11)$$

where  $\epsilon_{\text{metal}}$  is the complex dielectric constant of the metal at that wavelength (which is reported in refs 48 and 49) and  $\eta_{\text{eff}}$  is the effective index of refraction of the sample in question. The latter is measured experimentally (by comparing the observed SPR response to a calibration curve like Figures 3 and 4). Note that  $l_d$  varies only weakly with  $\eta_{\text{eff}}$ . For example, with a gold sensor film at a wavelength of 665 nm,  $l_d$  only decreases by 30% when  $\eta_{\text{eff}}$  decreases from the value of pure water (1.33) to that of a pure protein (1.57). It only decreases by 7% when a protein adsorbs from water to give an effective film thickness of 22 nm (i.e., several monolayers of protein).

It should be remembered that the use of a single value of  $l_d$  throughout the probe depth is really an approximation in bilayer and multilayer structures, since its value locally depends on the RI of the local medium. Such a local dependence could easily be incorporated into eq 3. However, it is not needed for most applications since (1)  $l_d$  varies only weakly with RI and (2) adlayer thicknesses are typically small compared to  $l_d$ . Thus, a single, average value of  $l_d$  in eqs 3–8 or eqs 12 and 13 below is usually suitable to provide adsorbed amounts that agree within 15% of that obtained from such a rigorous treatment. This more rigorous approach is only needed when the RIs in two different layers in the sample are different enough to give large differences in  $l_d$ , these two layers both have thicknesses that are larger than  $\sim 0.2l_d$ .

**IV.2. The SPR Response from Multilayer Film Structures.** In SPR sensor applications, it is common to have a trilayer structure of the type depicted in Figure 7, where adsorbate **b** is first used to attached a selective receptor to the metal surface, and adsorbate **a** is the analyte that subsequently binds thereupon from solution

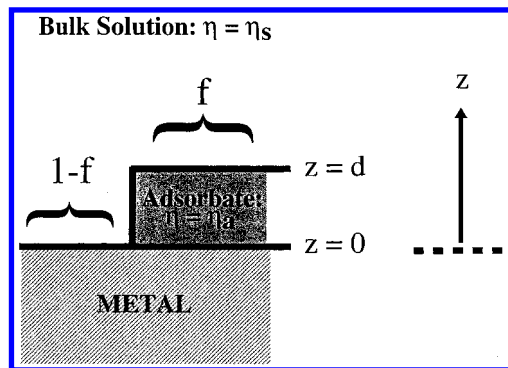


**Figure 8.** Schematic diagram of a bilayer structure with islanding, involving an adsorbate **a** of thickness  $d$  and refractive index  $\eta_a$  directly on the metal probe surface, but only covering a fraction  $f$  of its surface, above which is solution **s**, of refractive index  $\eta_s$ .

**s.** One might even have a multilayer structure with several different substances. Estimating the SPR response to such multilayer structures is a simple extension of eq 5a or 5b. Again, one simply uses eq 3 to calculate a properly weighted average refractive index for the multilayer structure and incorporate it into eq 2a or 2b. For the trilayer of Figure 7

$$\eta_{\text{eff}} = \eta_b [1 - \exp(-2d_b/l_d)] + \eta_a [\exp(-2d_b/l_d) - \exp\{-2(d_a + d_b)/l_d\}] + \eta_s \exp\{-2(d_a + d_b)/l_d\} \quad (12)$$

When substituted into eq 2a, this just gives

$$\Delta R = m(\eta_a - \eta_s) [1 - \exp(-2d_a/l_d)] \exp(-2d_b/l_d) \quad (13)$$

for the SPR response to the addition of the analyte film, **a**. (Here,  $\Delta R$  is defined as the SPR response only to the addition of **a**, after **b** was already present, and  $m$  is the slope of the calibration plot, taken in this range of  $\eta_{\text{eff}}$ .) Note the similarity of this expression to eq 5a: They differ only by the additional scaling factor of  $\exp(-2d_b/l_d)$  in eq 13. The SPR response to adding adlayer **a** is just the same as in the simpler case of species **a** alone, except that its magnitude is reduced by this factor due to the intermediate layer of **b**. When **b** is very thin compared to  $l_d$ , this factor is nearly 1.00, and the responsivity to **a** is unaffected by the intermediate receptor adlayer between the metal and **a**. On the other hand, when **b** is thicker than  $l_d$ , the sensitivity to **a** is severely decreased, dropping by a factor of  $\sim 7$  when the thickness of layer **b** is equal to  $l_d$ . When **b** is thick, the slope  $m$  may also be different than in the absence of **b**, but  $m$  is almost identical for thin **b**. Again, the use of a single value of  $l_d$  in eqs 12–13 is an approximation that is usually justifiable (see above).

**IV.3. Corrections for Nonuniformity in Coverage: Adsorbate Islands or Clusters.** Often, an adsorbate forms thick clusters on the surface rather than spreading uniformly across the sample. When the islands are comparable in thickness to  $l_d$ , or thicker, the SPR response to the adsorbate is not as strong as when uniformly spread. Consider the structure of Figure 8, where adsorbate **a** covers a fraction  $f$  of the metal surface in islands that are of thickness  $d$ . In this case the SPR response upon adsorption,  $R$ , is just  $f$  times the response when  $f = 1$  (i.e., for uniform coverage by a layer of the same thickness as the islands or clusters, for which equations are presented above). One can think of this system as having an effective index of refraction for the adlayer/solution structure, wherein weighted depth averaging is done as in eq 3, except that at each depth one

(48) Innes, R. A.; Sambles, J. R. *J. Phys. F: Met. Phys.* **1987**, *17*, 277.

(49) Palik, E. D., Ed. *Handbook of Optical Constants of Solids*; Academic Press: Orlando, FL, 1985.



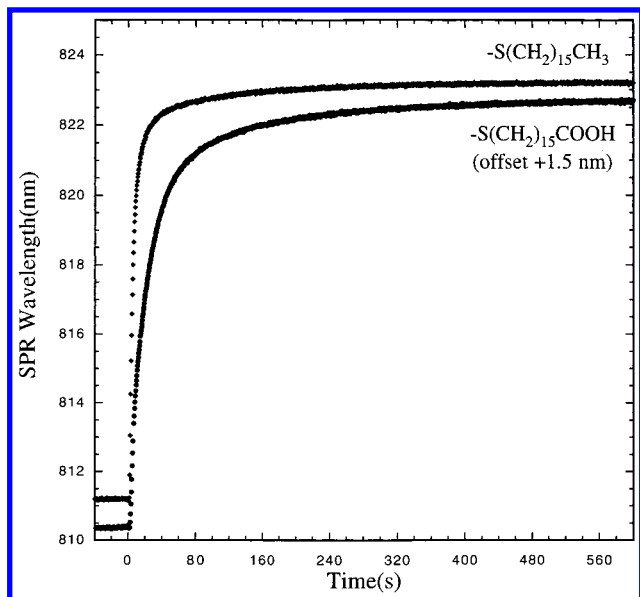


**Figure 9.** Response of the planar SPR to the adsorption of two thiolates, both from dilute ethanol solutions, at room temperature. Before time zero, pure ethanol was passing over the clean gold surface. At time zero, the solution was switched to one containing the thiol of interest in the following concentration: (a) 1.0 mM HS(CH<sub>2</sub>)<sub>15</sub>CH<sub>3</sub> and (b) 0.1 mM HS(CH<sub>2</sub>)<sub>15</sub>COOH.

must use an index of refraction which has been simply averaged over the surface area which is probed. (Such averaging parallel to the surface is actually only correct for island sizes that are small compared to the decay length of surface plasmons parallel to the surface, which is  $\sim 3 \mu\text{m}$ .<sup>50</sup> Large islands would give a complex SPR line shape with a double minimum that could only be interpreted from detailed analysis of the line shape.) The net result is that any of the material which is further from the metal surface than it would be if uniformly spread does not contribute as strongly to the SPR response, due to the exponential decay of the evanescent field. When the thickest parts of islands are still thin compared to  $l_d$ , the response to a certain volume of adsorbate in such islands is the same as it would be if that volume of adsorbate were spread over the entire surface in a uniform thickness as in Figure 1b. This would be the case for the adsorption of many proteins, each molecule of which can be thought of as an island of adsorbate, but still thin compared to  $l_d$ . For large adsorbates such as cells, a more complex treatment is needed, such as that in ref 37, which describes methods for treating various cell shapes within a related formalism (in which the decay length appears to be twice what we propose).

Again, when a preexisting adlayer b is already present on the metal surface, the SPR response to such a nonuniform adlayer,  $\Delta R$ , is just reduced by the factor  $\exp(-2a_b/l_d)$  similarly to eq 13. Thus, the SPR response to complex, nonuniform, and multilayer adlayer structures can very generally be estimated within this formalism.

## V. Comparison to Experiment: Measured SPR Response to Adsorbed Films

**V.1. Thiolate Adsorption on Gold.** Figure 9 shows the planar SPR wavelength response versus time upon exposure of the clean gold-coated glass slide, first to a solution of pure ethanol and then, at time  $t = 0$ , after switching to an ethanol solution containing (a) 1.0 mM

HS(CH<sub>2</sub>)<sub>15</sub>CH<sub>3</sub> and (b) 0.1 mM HS(CH<sub>2</sub>)<sub>15</sub>COOH. These thiol solutions are known to produce a self-assembled monolayer of the corresponding thiolate on the gold surface.<sup>29–34</sup> These are irreversibly bonded, as evidenced by the fact that the SPR wavelength after a 600 s exposure to these thiol solutions decreased by  $< 0.6 \text{ nm}$  when switched back to pure ethanol flow.

The thickness of the adlayers can also be estimated from the results of Figure 9 by using eq 6 (or eq 7 since these thicknesses are very small compared to  $l_d$ ). The SPR responses at saturation (after 250 s) upon adsorption of the  $-\text{CH}_3$ - and  $-\text{COOH}$ -terminated thiolates were 12.0 and 12.2 nm, respectively. Seven such uptake curves gave a standard deviation of 5% in the saturation response. From a calibration plot using toluene in ethanol solutions that cover the appropriate minimum wavelength range, we determined a sensitivity factor for this probe,  $m$ , of 7300 nm/RIU. The refractive index of the solvent, ethanol, is 1.361.<sup>40</sup> The RI of hexadecanethiol is estimated to be 1.463 (based on interpolation between reported values for other long-chain thiols<sup>40</sup>). The RI of the  $-\text{COOH}$ -terminated hexadecanethiol is estimated to be the same (1.463), since hexadecane and hexadecanoic acid have the same RI.<sup>40</sup> The adsorbed thiolates are estimated to have the same index of refraction as the corresponding bulk thiol (see above). The value of  $l_d$  is estimated to be  $\sim 0.41\lambda = 336 \text{ nm}$  from eq 11. Using these values in either eq 6 or 7 together with the measured SPR responses gives thiolate film thicknesses of 2.71 and 2.75 nm for the methyl-terminated and  $-\text{COOH}$ -terminated C<sub>16</sub> thiols, respectively.

These measured thicknesses estimated using our formalism can be compared to the known adlayer thicknesses based on prior literature. The packing density of these thiolate monolayers are known to be  $(4.4 \pm 0.2) \times 10^{14}$  molecules/cm<sup>2</sup>, based on prior radiolabeling<sup>34</sup> and structural studies.<sup>51</sup> This translates into films that are 2.2 and 2.3 nm thick in the case of the methyl-terminated and  $-\text{COOH}$ -terminated C<sub>16</sub> thiols, respectively, based on the bulk density of the corresponding thiol. (These are 0.85 and 0.92 g/cm<sup>3</sup>,<sup>40</sup> or  $1.98 \times 10^{21}$  and  $1.93 \times 10^{21}$  molecules/cm<sup>3</sup>, respectively. The density of HS(CH<sub>2</sub>)<sub>15</sub>-COOH was estimated by comparing those of hexadecane, hexadecanoic acid, and hexadecane thiol.) The thicknesses estimated with our formalism from the measured SPR response agree within 20–23% of these expected thicknesses. They agree similarly well with other measurements of the film thicknesses.<sup>13,27,31</sup>

**V.2. Protein Adsorption on Gold.** Serum albumin proteins are known to adsorb to a variety of surfaces from aqueous solution to make a nearly dense-packed monolayer with a packing density of  $\sim 2.5 \times 10^{-7} \text{ g/cm}^2$ .<sup>52</sup> By use of the specific volume of such proteins (0.77 cm<sup>3</sup>/g<sup>24,45,46</sup>), this corresponds to an effective film thickness of pure protein of  $\sim 1.9 \text{ nm}$ . The SPR response to binding of the protein bovine serum albumin (BSA) to a clean gold surface on the planar probe is shown in Figure 10. The SPR response observed after adsorption for 800 s, where a saturation coverage is approached, is 8.0 nm in wavelength, with a reproducibility of 0.3 nm.

The measured protein film thickness can be calculated from this response using eqs 5a, 6, or 7 and the following constants. Albumin proteins have an index of refraction of 1.57 (see above), compared to 1.334 for the aqueous

(51) Li, J.; Liang, K. S.; Camillone, N. I.; Leung, T. Y. B.; Scoles, G. *J. Chem. Phys.* **1995**, *102*, 5012.

(52) Fair, B. D.; Jamieson, A. M. *J. Colloid Interface Sci.* **1980**, *77*, 525.

(50) Berger, C. E. H.; Kooyman, R. P. H.; Greve, J. *Rev. Sci. Instrum.* **1994**, *65*, 2829.

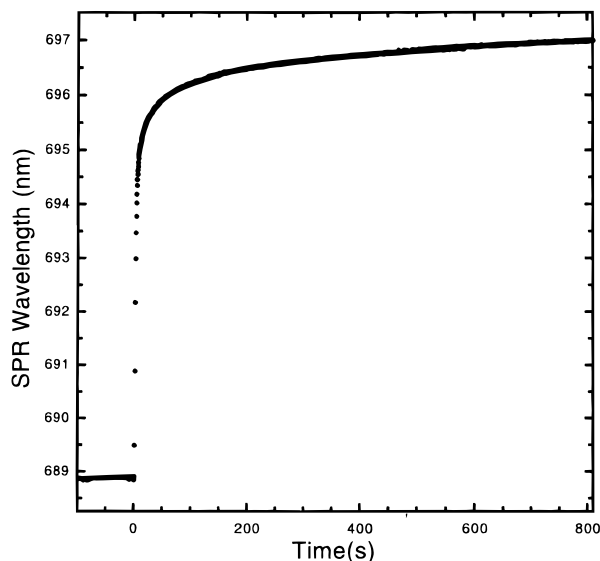


**Figure 10.** Response of the planar SPR to the adsorption of the protein BSA (bovine serum albumin) from dilute aqueous buffer solution (1 mg/mL in PBS buffer at pH 7.0), onto the clean gold surface of the SPR probe at room temperature.

buffer solution used to dose this protein. The SPR sensitivity factor over this range was determined by calibration to be 3100 nm/RIU (Figure 3). We get from eq 11 that  $l_d = \sim 0.34\lambda = 233$  nm. The observed SPR response of 8.0 nm near saturation (i.e., after 800 s) thus gives an observed adlayer effective thickness of 1.3 nm using either eq 5a, 6, or 7. This converts to a protein concentration on the surface of  $1.71 \times 10^{-7}$  g/cm<sup>2</sup>. This is 32% below the estimated close-packed coverage of  $\sim 2.5 \times 10^{-7}$  g/cm<sup>2</sup> (or thickness of  $\sim 1.8$  nm), which itself is probably only accurate to  $\sim 30\%$ .<sup>52</sup> A smaller value may be found because of the very short adsorption time used here (800 s), at which the adsorbed amount is still increasing very slowly (see Figure 10). Note that in studies of BSA adsorption on gold surfaces that were prefunctionalized with a wide variety of organic thiols, and on a variety of polymer surfaces, the most adsorptive surfaces showed very similar saturation coverages of BSA ( $(1.2\text{--}1.8) \times 10^{-7}$  g/cm<sup>2</sup>).<sup>23,47</sup>

Note that this measured thickness of 1.3 nm is the average effective thickness of pure protein, and it will be considerably less than the optical thickness measured in ellipsometry and some applications of SPR. That optical thickness generally includes a great deal of water that fills the voids between proteins,<sup>47,53–55</sup> which also results in a smaller “effective index of refraction” than that for pure proteins.<sup>47</sup> Quantitative determination of the amount of adsorbed protein (in ng/cm<sup>2</sup> or molecules/cm<sup>2</sup>) is best done using the effective thickness of pure protein as we do, since its index of refraction and specific volume are known constants and since the amount of water included in the protein film will vary greatly between different proteins and different surfaces. If the optical thickness approaches  $l_d$ , however, one must include a factor  $f$  discussed in section IV.3 to take into account the volume fraction of water in the adlayer. At smaller thicknesses, the factor  $f$  can be ignored without loss in accuracy since the weight of adsorbed protein calculated from the SPR

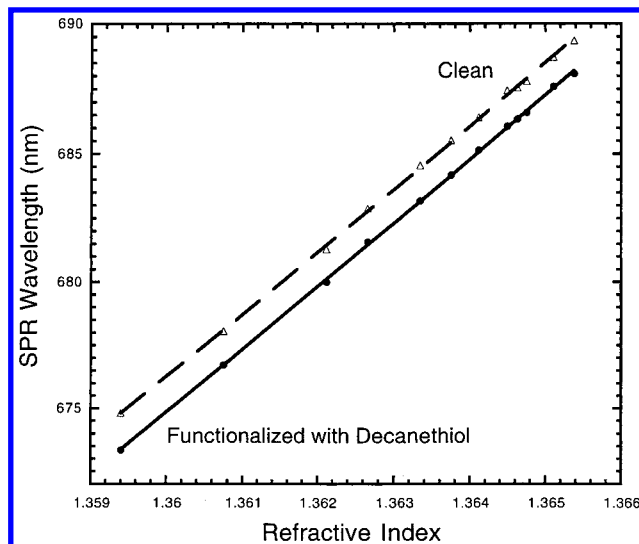


**Figure 11.** Measured SPR response (wavelength of minimum in the reflected light intensity) versus the bulk index of refraction ( $\eta$ ) of solutions in contact with the gold SPR fiber-optic probe surface, with and without prefunctionalization with a decane thiolate adlayer (like those in Figure 9). Room temperature.

response will be independent of  $f$ , and therefore estimation of  $f$  is not necessary.

**V.3. Influence of a Prefunctionalizing Film on the Measured Response.** Equation 13, which is used for predicting thicknesses of bilayer structures, is supported by the experimental results shown in Figure 11. Here, the response of the fiber optic SPR system was measured as a function of changes in the index of refraction of bulk solutions in contact with the gold, both with and without an intermediate prefunctionalizing layer of decanethiolate. The thiolate adlayer has a negligible effect on the response slope, which is within 0.7% of 2466 nm/RIU in both cases and, therefore, well within the reproducibility in determining the slope ( $\sim 2\%$ ).

In applying eq 13, the decanethiolate can be considered as layer **b** (see Figure 7) with a thickness  $d_b$  of  $\sim 1.5$  nm based on its packing density ( $4.4 \times 10^{14}$  thiolates/cm<sup>2</sup>, see above) and the bulk density of the corresponding thiol (0.844 g/cm<sup>3</sup>).<sup>40</sup> The bulk solution can be considered as an infinitely thick layer of **a**. In this case, eq 13 reduces to

$$\Delta R = m(\Delta\eta) \exp(-2d_b/l_d) \quad (14)$$

where  $\Delta\eta$  refers to the change in index of refraction of **a**, and  $\Delta R$  refers to the corresponding SPR response. While this thiolate would cause a change in the wavelength of the SPR minimum for any given bulk index of refraction above it, as described above, this change is constant so that the slopes of the two curves in Figure 11 are the same. This is because the factor  $\exp(-2d_b/l_d)$  in eqs 13 and 14 is nearly unity when  $d_b$  is so small compared to  $l_d$  ( $\sim 300$  nm).

In principle, the offset between the two curves can be predicted using eq 5a or 7, since the thiolate adlayer in this case is expected to be  $\sim 1.5$  nm thick. However, these two curves were collected 3 days apart, and the fiber optic probe was moved through air to another beaker between these measurements. This causes baseline changes that are large relative to the shift due to thiolate adsorption, so this comparison is meaningless for these particular data.

(53) Corsel, J. W.; Willems, G. M.; Kop, J. M. M.; Cuyper, P. A.; Hermens, W. T. *J. Colloid Interface Sci.* **1986**, *111*, 544.

(54) Sundgren, J.-E.; Bodó, P.; Ivarsson, B.; Lundström, I. *J. Colloid Interface Sci.* **1986**, *113*, 530.

(55) Prime, K. L.; Whitesides, G. M. *J. Am. Chem. Soc.* **1993**, *115*, 10714.

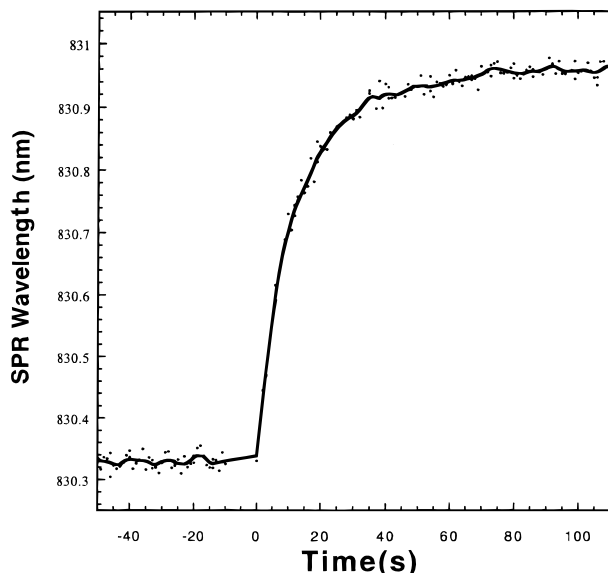
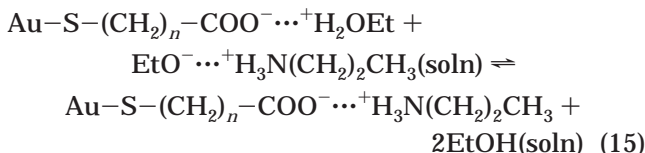


**Figure 12.** Response of the planar SPR, prefunctionalized with  $-\text{S}(\text{CH}_2)_{16}\text{COOH}$  as in Figure 9, to the adsorption of propylamine from dilute ethanol solution (2.4 mM) at room temperature.

**V.4. Propylamine Adsorption on  $-\text{COOH}$  Prefunctionalized Gold.** The response of the planar SPR spectrometer to the binding of *n*-propylamine in ethanol solution to a  $-\text{COOH}$  prefunctionalized gold surface is shown in Figure 12. The gold surface was prefunctionalized with a  $-\text{COOH}$ -terminated thiolate self-assembled monolayer as described in section II (which is similar to that in Section V.1, but with a longer reaction time). A driving force for the observed reversible binding reaction of the protonated amine to this surface should be similar to the binding reaction occurring at the  $-\text{COOH}$ -terminated resin surface of ion exchange columns and that occurring in poly-L-lysine adsorption from aqueous solution<sup>56,57</sup> and alkylamine adsorption from the gas phase<sup>58,59</sup> on similar  $-\text{COOH}$ -terminated thiolate self-assembled monolayers on gold. In solutions, the species are mostly ionic and solvated, and the cations are held to the anionic surface by weak electrostatic interactions



Basic conditions help drive this class of reaction,<sup>56</sup> which may help explain why it is observed under the present conditions but not with a lysine monomer in water at  $\text{pH} = 8.5$ .<sup>56</sup>

The saturation change in the SPR wavelength minimum in Figure 12 is  $\sim 0.68$  nm (with a reproducibility within 0.04 nm based on other runs), and the calibration of this probe in this range gave a sensitivity factor of 7400 nm/RIU. From eq 5a, 6, 7, or 13, this saturation response gives a propylamine monolayer thickness of 0.63 nm using that  $\eta_a = 1.387$  and  $\eta_s = 1.361$ <sup>40</sup> and that  $l_d = 358$  nm =

$0.43 \lambda$  from eq 11. Using the bulk liquid density of this molecule ( $0.7173$  g/cm<sup>3</sup>) and assuming simple cubic packing in the bulk gives a size for propylamine of 0.52 nm (or the edge length of the "cubes"), very close to this measured monolayer thickness. The measured thickness corresponds to a coverage of propylamine of  $4.6 \times 10^{14}$  molecules/cm<sup>2</sup>, again using the bulk density. The surface concentration of the  $-\text{COO}-$  headgroups is  $\sim 4.4 \times 10^{14}$ /cm<sup>2</sup> (see above). One expects a 1:1 stoichiometry for the binding reaction, so the expected surface coverage at saturation is  $\sim 4.4 \times 10^{14}$  molecules/cm<sup>2</sup>. Again, the measured saturation coverage is very close to that expected.

## VI. Detection Limits

**VI.1. Measured Detection Limits for Bulk Indices of Refraction.** The detection limits for the planar system based on the scatter in the SPR wavelengths in Figure 3 ( $\sim 0.01$  nm) is about  $3 \times 10^{-6}$  RIU for the large time span of those measurements. Experiments with the flow cell wherein a quicker change in solution was accomplished using a chromatographic sampling valve showed that changes of  $\sim 0.007$  nm in wavelength or  $2 \times 10^{-6}$  in RIUs could be detected easily when occurring within a few minutes time. With the SPR fiber-optics probe, a detection limit of  $< \sim 0.03$  nm in wavelength or  $1 \times 10^{-5}$  in RIUs was found by stepwise additions of solute to the beaker of solution. The SPR detection limits for changes in bulk index of refraction depend on the noise and baseline drift in the wavelength of the SPR minimum, as well as the magnitude of  $m$ , the slope of wavelength versus RI. The noise can be reduced by signal averaging, but baseline drift can be a problem. Slow measurement generally degrades the detection limit, since baseline drift becomes increasingly problematic with increasing time. Comparable detection limits ( $2 \times 10^{-6}$  to  $1 \times 10^{-5}$  RIU) have been reported previously.<sup>14-16</sup>

The detection limit of the planar device was not significantly affected by using a variety of different preparation methods for the gold films as long as their thickness was maintained close to 50 nm. The major factor influencing detection limits was baseline stability, which for the planar sensor was limited by temperature drift, we believe. The fiber optic probe was less stable, perhaps due to interactions of the probe fluid with the fiber/cladding interface. Mechanical stability of any index-matching fluid interfaces is also quite important. The thickness of the gold film influences the calibration slope,  $m$ , especially at high RI. Neither slope nor detection limit degrade significantly with time unless the surface becomes heavily contaminated.

**VI.2. Detection Limits for Surface Concentrations and Adlayer Thicknesses.** For a single adlayer of uniform thickness, one can easily predict a detection limit for that thickness,  $d_{\text{min}}$ , based on the detection limit for changes in bulk index of refraction in the absence of that film. We showed above that our planar system has a detection limit of  $\sim 2 \times 10^{-6}$  RIU, which according to the above discussion can be set equal to  $(\eta_a - \eta_s)(2d_{\text{min}}/l_d)$ . Thus, the detection limit is  $(1 \times 10^{-6}) l_d$  divided by the RIU difference between the adsorbate and solution. For a typical value of  $l_d$  of 300 nm and  $(\eta_a - \eta_s) = 0.1$ , this gives a detection limit of 0.003 nm or 0.03 Å in average film thickness. Since a typical atom is  $\sim 2$  Å in diameter, this corresponds to only  $\sim 1.5\%$  of a single atomic layer. As described above, the thickness detection limit can easily be converted to a coverage detection limit (molecules/cm<sup>2</sup>) by multiplying by the bulk density of the adlayer in

(56) Jordan, C. E.; Corn, R. M. *Anal. Chem.* **1997**, *69*, 1449.

(57) Jordan, C. E.; Frey, B. L.; Kornguth, S.; Corn, R. M. *Langmuir* **1994**, *10*, 3642.

(58) Yang, H. C.; Dermody, D. L.; Xu, C.; Ricco, A. J.; Crooks, R. M. *Langmuir* **1996**, *12*, 726.

(59) Matsuura, K.; Ebara, Y.; Okahata, Y. *Thin Solid Films* **1996**, *273*, 61.



molecules/cm<sup>3</sup>. If the sensor is precoated with another adlayer, these detection limits would be increased by the factor  $\exp(2d_b/\lambda)$  as follows from the derivation of eq 13. This factor is nearly unity when  $d_b$  is very small compared to  $\lambda$ . If the molecule is exceedingly nonuniformly spread across the surface with severe clustering, this detection limit could be increased as well, as also follows from the discussion above.

A detection limit of  $\sim 6\%$  of a monolayer of propylamine, or  $<0.04$  nm average film thickness, can be seen from the raw data points in Figure 12. In this case the difference in index of refraction between the adsorbate and the solution is only 0.026 RIU. For a more typical difference of 0.1 RIU, this corresponds to a detection limit of  $\sim 0.01$  nm in film thickness. For protein adsorption in aqueous buffer, where the difference is  $\sim 0.24$  RIU, it corresponds to a detection limit of 0.004 nm thickness, or 0.5 ng/cm<sup>2</sup>, or  $\sim 2 \times 10^{-3}$  monolayers. Data smoothing would improve this considerably, but at the cost of poorer time resolution. (The response time to a step change in bulk index of refraction was  $<2$  s under the conditions of Figure 12.)

Kunz et al.<sup>14</sup> discussed the detection limits of planar and fiber-optic SPR devices in terms of bulk index of refraction changes and bulk analyte concentrations, but not in terms of adsorbate coverages or thicknesses. From Maxwell's equations, Yeatman<sup>15</sup> estimated a detection limit of  $3 \times 10^{-6}$  RIU, or 3 nm thickness for an adsorbate whose index of refraction was 0.1 RIU different than the surrounding medium, for certain characteristics of the SPR spectrometer. A detection limit of  $\sim 0.1$  nm thickness was estimated by Häussling et al.<sup>17</sup> We show thickness detection limits significantly better than either of these estimates, although in the former case it may be just an interpretation difference.

**VI.3. Detection Limits for Bulk Concentrations of Analytes in Solutions.** In adsorption-based chemical sensors or in immunoassays, one is generally more interested in the detection limits in terms of the bulk solution concentration of the analyte, antigen, or antibody. Connecting to these units from a detection limit in units of adlayer effective thickness or surface coverage is nontrivial, since the conversion factor depends on the equilibrium constant,  $K_{eq}$ , for binding of the analyte to the sites on the SPR surface, which may not be known. If it is known, then one can use its definition to estimate the detection limit in units of bulk concentration. Consider the simplest binding reaction



where A is the solution phase analyte and S is its surface site in a prefunctionalized adlayer on the sensor surface. The equilibrium constant is defined as

$$K_{eq} = [A-S]/\{[A][S]\} = \theta/\{(1 - \theta)[A]\} \quad (16)$$

where [A] is the concentration of the analyte and  $\theta$  is the fraction of its sites that are occupied at equilibrium. If the adlayer system is well designed,  $\theta$  will be small at the detection limits, so that  $(1 - \theta)$  is  $\sim 1.00$ . In this case,  $[A] = \theta/K_{eq}$ . Thus, the detection limit for the bulk concentration of A will just be the detection limit for the fraction of its bound sites divided by  $K_{eq}$ . The detection limit for the fraction of its bound sites can be estimated as described above: First estimate the coverage detection limit (molecules/cm<sup>2</sup>) and then divide that number by the number of binding sites per cm<sup>2</sup> in the prefunctionalized layer. The number of binding sites per cm<sup>2</sup> can be estimated by

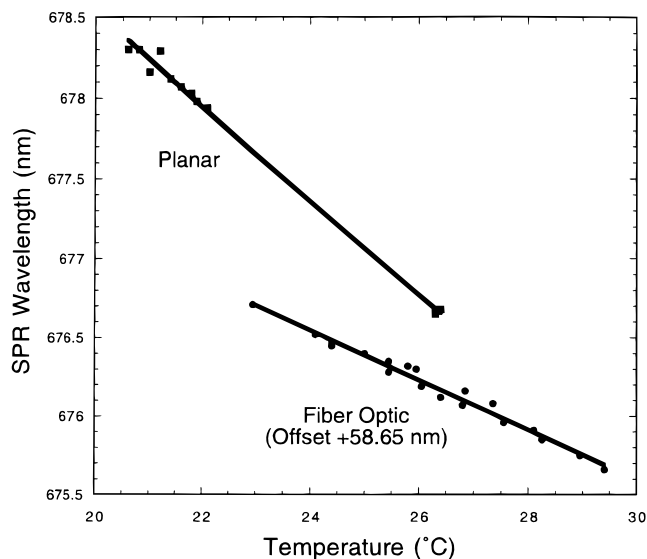


**Figure 13.** Temperature dependence of the SPR response in water, for both the planar (squares) and fiber-optic (circles) SPR sensors. The fiber-optic data have been uniformly shifted vertically to bring onto the same scale.

measuring the saturation coverage at high concentration of A using the SPR response and the procedures outlined above.

While one often knows the equilibrium constant for the analogous reaction where the sites S are dissolved in solution, the way in which S is immobilized onto the sensor surface may alter the value of  $K_{eq}$ . It is best to make separate measurements of the equilibrium constant for the surface-immobilized S, which can be done by using the SPR itself to measure  $\theta$  versus [A].

**VI.4. Temperature Sensitivity and Its Effect on Detection Limits.** To achieve Figures 3 and 4 and the above-stated detection limits, we controlled the temperatures of the solutions to some extent, since we found that the baseline drifted sensitively with changing temperature. The SPR response to changes in temperature for water solutions of fixed composition (pure water) are plotted in Figure 13, for both the planar and fiber-optic spectrometers. As can be seen, the wavelength minimum decreases by about 0.29 and 0.16 nm per degree Kelvin for the planar and fiber-optic probes, respectively. The refractive index of water is known to decrease by  $\sim 8 \times 10^{-5}$  RIU per degree K near room temperature.<sup>40</sup> Ignoring the changes associated with temperature effects on the solid parts of the SPR probe, and using the sensitivity factors of 3100 and 1600 nm/RIU, respectively, from above, one would predict a slope of  $(-8 \times 10^{-5} \text{ RIU/K}) \times (3100 \text{ nm/RIU}) = -0.25 \text{ nm/K}$  for the planar probe and  $-0.13 \text{ nm/K}$  for the fiber-optic probe, very close to the observed slopes. This suggests that the dominant effect of temperature is in its effect on the refractive index of the liquid solution. This is expected, since the index of refraction of the liquid (water here) will typically change much more sensitively with temperature than that for solids. From the above discussion, it is obvious that the temperature of the liquid must be controlled to better than  $2 \times 10^{-2}$  K over the time scale of the two measurements to achieve detection limits of  $2 \times 10^{-6}$  RIU or  $\sim 0.003$  nm in thickness.

## VII. Conclusions

We have outlined here a procedure for estimating structural parameters of adsorbed layers (thickness, surface concentration, or fractional coverage) based on

measured SPR responses. All that is needed is a knowledge, through calibration, of the SPR response versus bulk index of refraction, and absolute thicknesses can be estimated using this method with reasonable absolute accuracy and very high relative accuracy and precision. That is, no calibration versus adlayer thickness is required with this method, although such a calibration would improve the absolute accuracy. In this method, the index of refraction of the adlayer must be assumed, but we outline here ways for estimating it. The method is tested on several thin adlayers of known thickness, and an absolute accuracy within  $\sim 25\%$  is obtained. The accuracy is limited by inaccurate knowledge of the penetration depth of the SPR evanescent field and the index of refraction of the adlayer. It is a useful quantitative method for adlayers up to  $>200$  nm in thickness. It is shown that, if the SPR is capable of detecting changes in bulk index of refraction of  $2 \times 10^{-6}$  RIU, as is the planar system described here, then the detection limit for adsorbed layers is a thickness of only  $\sim 3 \times 10^{-4}$  nm RIU, divided by the difference in index of refraction between the adsorbate and the dosing solution. This typically gives a limit below  $10^{-2}$  nm, or

$0.1 \text{ \AA}$  average thickness. The dynamic range is therefore rather large, from  $\sim 10^{-2}$  to  $>200$  nm in average film thickness.

Methods are also presented for correcting the quantitative estimates of adsorbate coverage or adlayer thickness for the presence of a prefunctionalizing adlayers (for example, due to a receptor adlayer on the sensor) and for nonuniformities in the thickness of the adlayer across the SPR probe area.

**Acknowledgment.** The authors acknowledge Texas Instruments, the Department of Energy Office of Basic Energy Sciences (Chemical Sciences Division), the UWEB NSF Engineering Research Center Grant EEC-9529161, and the University of Washington's Center for Process Analytical Chemistry for partial support of this work. They thank P. Stayton, K. Nelson, T. Sasaki and M. Boekel for providing some of the chemical reagents used here, Gabriel Lopez for critical reading of the manuscript, and Alex Engel for technical assistance.

LA971228B